

shows the 0.4" J/H/K SHARP images (Table 1), as well as a 0.6" J-K colour map (Tacconi-Garman et al. 1993, Genzel et al. 1994). Outside of the Seyfert nucleus (90 mJy at K) there is a 1.5" radius, ring structure with embedded knots. The colours of the ring are consistent with a stellar cluster reddened by $A_V \approx a$ few; in contrast, the very red nuclear colours suggest hot dust emission, as in the case of NGC 1068. The near-infrared images of Figure 4 are in very good agreement with similar resolution visible speckle images (Mauder et al. 1994) and with a VLA map of the 5 GHz radio emission (Wilson et al. 1991). All these data and $\approx 0.9''$ near-infrared spectral line imaging with the MPE FAST spectrometer fit a model in which the ≈ 500 pc ring is powered by a luminous starburst forming about $50 M_\odot$ of new stars per year for the last 1 to 3×10^7 years (Weitzel et al. 1994). One supernova explosion every two years is implied and may be detectable by means of time variability in the high-resolution near-infrared maps. The triggering mechanism for the circum-nuclear burst in NGC 7469 remains unclear as, in contrast to NGC 1068, the SHARP data do not show evidence of a bar structure. Perhaps the burst was triggered by the interaction of NGC 7469 with its neighbour, IC 5283.

The data we have presented in this report only represent a selection of a sample of about a dozen galaxies that have been observed so far with SHARP. We believe that this brief glimpse already demonstrates the power of the new tool of subarcsecond near-infrared imaging. The future is clearly bright.

Acknowledgements. We would like to thank Harry van der Laan for giving us the opportunity to bring SHARP to the right place at the right time.

References

- Antonucci, R.R.J. and Ulvestaad, J.S. 1988, *Ap.J.* **330**, L97.
- Bedding, T.R., von der Lühe, O., Zijlstra, A.A., Eckart, A. and Tacconi-Garman, L. 1993, *The Messenger* **74**, 2.
- Blietz, M. et al. 1994, *Ap.J.* **421**, in press.
- Cameron, M. et al. 1993, *Ap.J.* **419**, 136.
- Canzian, B., Mundy, L.G. and Scoville, N.Z. 1988, *Ap.J.* **333**, 157.
- Christou, J.C. 1991, *Exp. Astr.* **2**, 27.
- Eckart, A., Hofmann, R., Duhoux, P., Genzel, R. and Drapatz, S. 1991, *The Messenger* **65**, 1.
- Eckart, A., Genzel, R., Krabbe, A., Hofmann, R., van der Werf, P.P. and Drapatz, S. 1992, *NATURE* **335**, 526.
- Eckart, A., Genzel, R., Hofmann, R., Sams, B.J. and Tacconi-Garman, L.E. 1993, *Ap.J.* **407**, L77.
- Eckart, A., van der Werf, P.P., Hofmann, R. and Harris, A.I. 1994, *Ap.J.* April issue.
- Gallais, P. 1991, PhD Thesis (Paris: University of Paris).
- Genzel, R. and Eckart, A. 1994, in *Infrared Astronomy with Arrays* (3), ed. I. McLean and G. Brims (Dordrecht: Kluwer), in press.
- Genzel, R. et al. 1994, in prep.
- Haniff, C.A. and Buscher, D.F. 1992, *J.Opt. Soc.Am.* **9**, 203.
- Knox, K.T. 1976, *J.Opt.Soc.Am.* **66**, 1236.
- Krabbe, A., Sternberg, A. and Genzel, R. 1994, *Ap.J.* in press.
- Lohmann, A.W., Weigelt, G. and Winitzer, B. 1983, *Appl.Opt.* **22**, 4028.
- Lucy, L.B. 1974, *A.J.* **79**, 745.
- Mauder, W., Weigelt, G., Appenzeller, I. and Wagner, S.J. 1994, *Astr.Ap.* in press.
- Rieke, G.H., Lebofsky, M.J., Thompson, R.I., Low, F.J. and Tokunaga, A.T. 1980, *Ap.J.* **238**, 24.
- Saikia, D.J. et al. 1990, *MNRAS* **245**, 397.
- Sams, B.J., Genzel, R., Eckart, A., Tacconi-Garman, L.E. and Hofmann, R. 1994, *Ap.J.* (Let.) in press.
- Sersic, J.L. and Pastoriza, M. 1965, *PASP* **77**, 287.
- Tacconi-Garman, L.J., Eckart, A., Genzel, R. and Sternberg, A., 1993, *BAAS* **25**, 1338.
- Tacconi-Garman, L.J. et al. 1994, in prep.
- Telesco, C. and Decher, R. 1988, *Ap.J.* **334**, 573.
- Véron-Cetty, M.-P. and Véron, P. 1983, *The Messenger* **34**, 22.
- Weitzel, L. et al. 1994, in prep.
- Wilson, A.S., Helfer, T.T., Haniff, C.A. and Ward, M.J. 1991, *Ap.J.* **381**, 79.

Infrared Spectroscopy of Galactic Globular Clusters

L. ORIGLIA¹, A.F.M. MOORWOOD² and E. OLIVA³

¹Osservatorio Astronomico, Pino Torinese, Italy; ²ESO; ³Osservatorio Astrofisico, Firenze, Italy

1. Introduction

Galactic globular clusters (GGCs) are the best templates for studying the physical and chemical properties of old stellar systems at different evolutionary stages. Zinn (1985) distinguishes two main subsamples on the basis of their spatial distribution, kinematics and metallicity; the halo system characterized by low rotational velocity and metallicity ($[\text{Fe}/\text{H}] \leq -0.8$) and large velocity dispersion, and the disk+bulge system which is metal-rich ($[\text{Fe}/\text{H}] > -0.8$) and exhibits a large rotational velocity and lower dispersion.

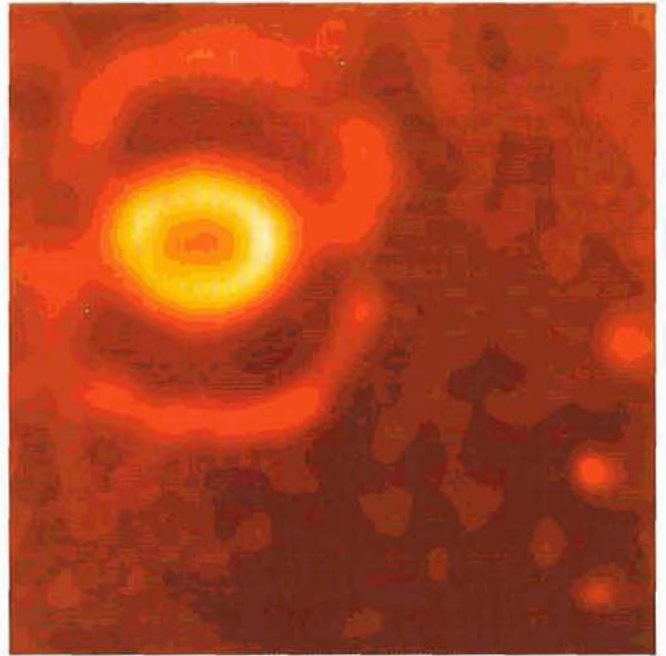
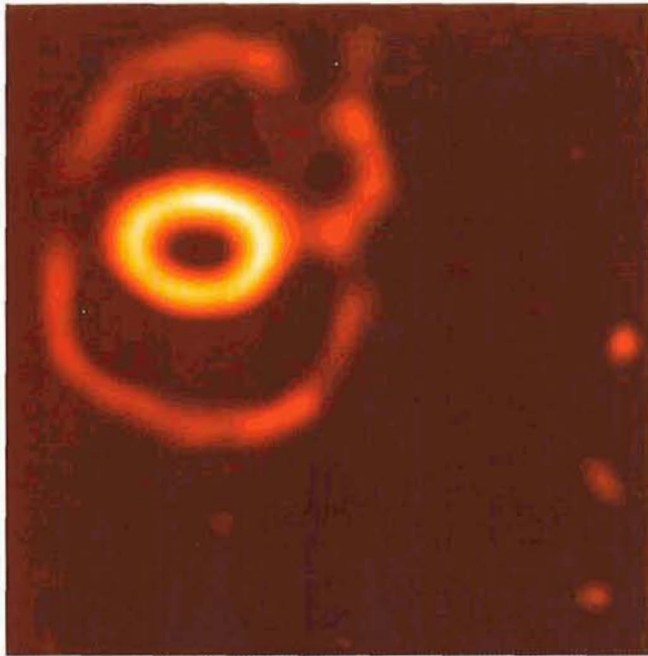
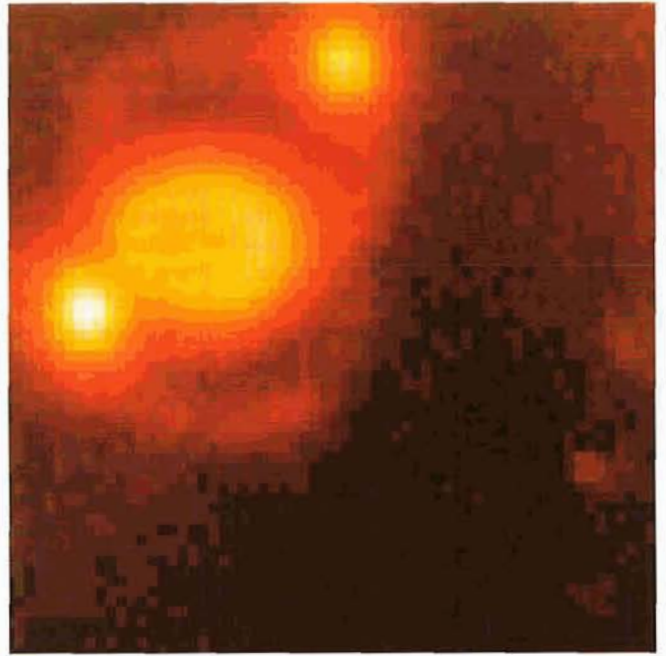
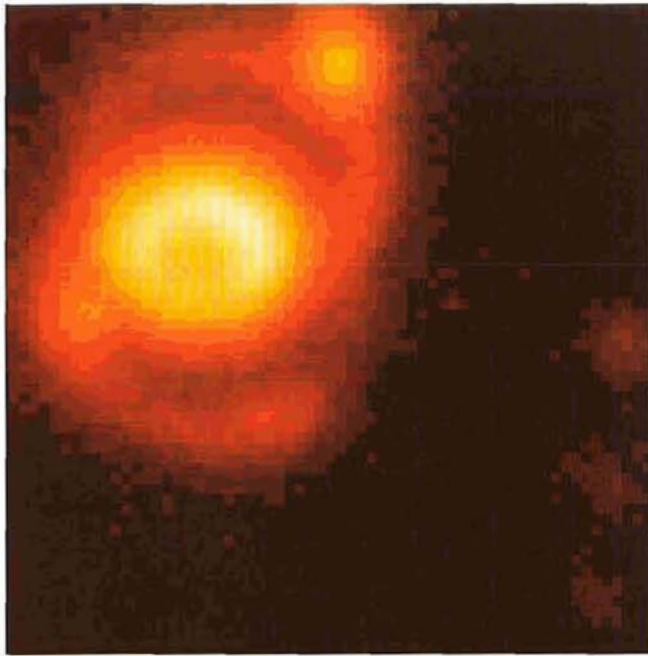
From theoretical models (Renzini and Buzzoni 1986, Chiosi et al. 1986) it is expected that the integrated luminosity of old stellar populations is dominated by the luminous red giant branch (RGB) stars which are close to the He-flash.

This scenario is largely confirmed by photometric and spectroscopic optical/infrared observations of the central regions and of the brightest single stars in many clusters (see for example Frogel et al. 1983a, b and references therein). The average temperature of this red and cool stellar component, i.e. the location of the red giant branch in the HR diagram, is directly related to the metal content of the cluster; the higher $[\text{Fe}/\text{H}]$ the cooler the stars (Frogel et al. 1983b). Therefore, any temperature sensitive index (e.g. V-K, photometric CO) could, in principle, be used to determine the metallicity of globular clusters. The main limitations in the use of photometric indexes are extinction and contamination by foreground stars and both effects are particularly important when studying high metallicity clusters in the bulge. A

way to overcome these problems is to use spectroscopic indices (which are intrinsically unaffected by extinction) in the infrared where the contamination from foreground stars is much less important than in the optical. We use two spectral indices in the infrared H band centred on SiI+OH 1.59 μm and CO(6-3) 1.62 μm together with the "classical" CO(2-0) 2.29 μm feature. These indices are good temperature indicators in cool stars (Origlia et al. 1993).

In this article we present integrated spectra of these features for a sample of GGCs and show that diagrams based on their equivalent widths can be used to tightly define the metallicity sequence from metal poor halo clusters to the most metal rich in the disk+bulge.

(continued on page 23)



New NTT Images of SN 1987A

H- α and N II $\lambda 6584$ images of the nebulosities near SN 1987A that were taken by the NTT on December 19, 1993. H- α images are on the right and N II images are to the left. The upper image of each pair is the raw image while the lower is after deconvolution using the Lucy-Richardson image restoration technique (ESO preprint #975). All images are shown with a logarithmic intensity scale and they are oriented so that north is up and east is to the left. The CCD pixel size in the original image is 0.129 arcsec/px. The filter bandpasses were $\sim 10\text{\AA}$ and the wavelengths were centred to be correct for the redshift of the Supernova. The seeing for the N II image was about 0.7 arcsec (FWHM), and for the H- α image it was about 0.8 arcsec (FWHM). The resolution of the deconvolved image is ~ 0.2 arcsec (FWHM) for the N II image, and it is ~ 0.3 arcsec (FWHM) for the H- α image. In the deconvolved images the flux from star 2 (NW of the inner loop) and star 3 (SE of the loop) have been compressed into single pixels (white dots) at the locations of the star images. The deconvolution procedure produces some "ringing" around bright objects. In the deconvolved images, ringing caused by the inner loop and the two bright companion stars has caused breaks in the very faint outer loops and distortions in the intensity profile near the inner loop.

Note that in the raw N II image star 2 is much brighter than star 3, but that in the H- α image star 3 is much brighter than star 2. This is because star 3 is a Be star with strong H- α emission while star 2 has H- α absorption in its spectrum. The middle star in the line of three stars along the SW edge of the pictures is a close double. The intensity distribution of light around the inner loop is different in H- α from that of N II. Also, while the SE portion of the inner loop is now fading, the bright portions are now increasing in brightness (IAU Circular #5927). It seems likely that interactions between the expanding SN envelope and diluted gas within the inner loop are generating UV photons that are beginning to reionize the nebula.

L.-F. WANG and E.J. WAMPLER

Figure 1: Spectra centred at 1.59, 1.62 and 2.29 μm of the selected galactic globular clusters in the halo (top panel) and in the disk (bottom panel). The equivalent widths W are in \AA and the metallicities are given in the lower right hand corners.

2. Observations and Data Reduction

The data were collected during several observing runs (June 1991, November 1992, April and October 1993) at the ESO NTT telescope using the IRSPEC infrared spectrometer (Moorwood et al. 1991) equipped with a SBRC 62×58 InSb array detector. The pixel size was 2.2 arcsec along the slit and $\approx 5 \text{\AA}$ along the dispersion direction yielding a resolving power $R \approx 1500$ with a 2 pixel ($4.4''$) slit.

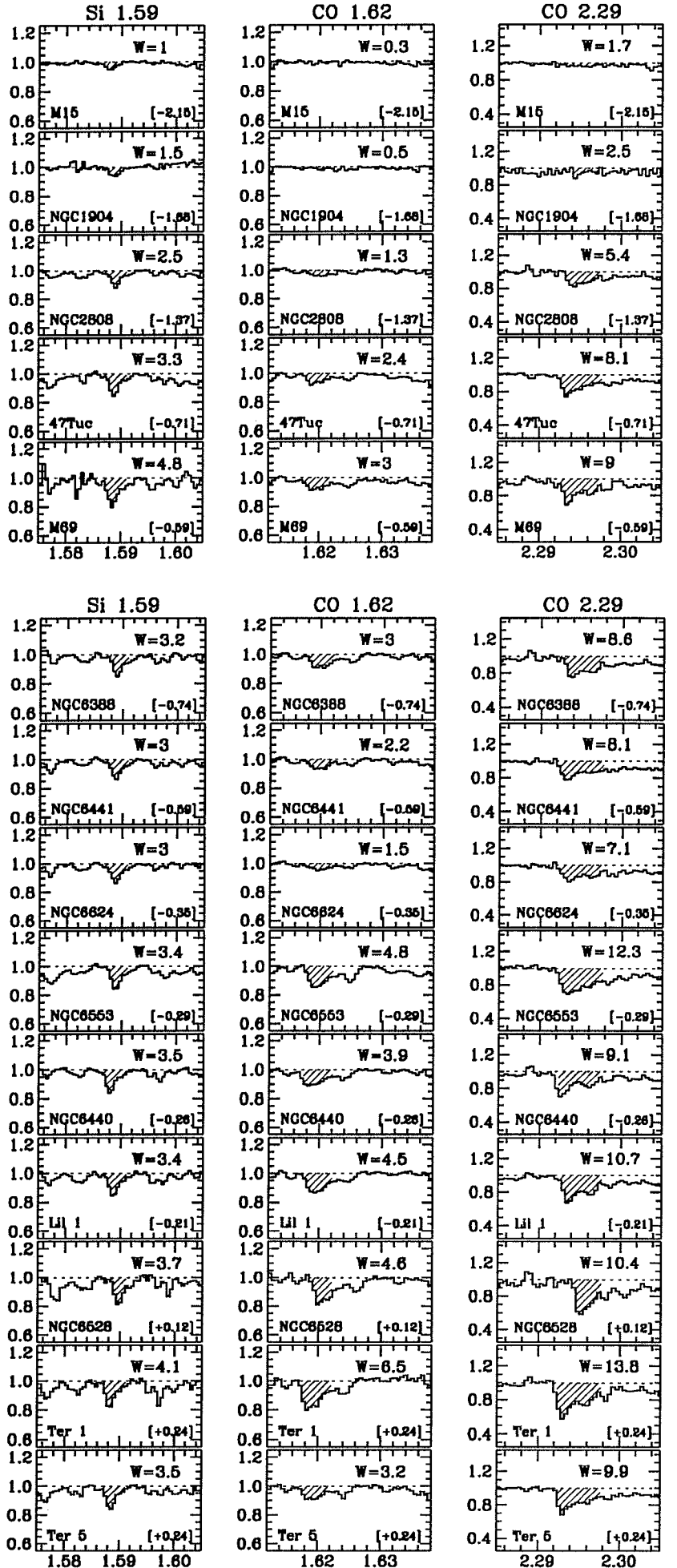
Deep, long-slit spectra centred at 1.59 (Si), 1.62 (CO 6-3), and 2.29 (CO 2-0) μm of a sample of galactic globular clusters in the halo and in the disk were obtained. The total average integration time was 16 minutes (sources+sky) for each grating position with automatic telescope beam switching every 2 minutes. The instrumental and atmospheric responses were corrected using reference spectra of featureless O5-6 stars. Data reduction was performed using the IRSPEC context of MIDAS and more details about IRSPEC reduction can be found e.g. in Origlia et al. (1993).

3. Results and Discussion

Normalized spectra of the central region (about $6'' \times 4''$ centred on the core) of the observed clusters are displayed in Figure 1. The shaded areas correspond to the measured equivalent widths in \AA given on each spectrum which were computed using the procedure described in Origlia et al. (1993).

In Figure 2 we plot the measured equivalent widths in spectroscopic equivalents of colour-magnitude diagrams, i.e. 1.62 vs 1.62/1.59 and the 1.62 vs 1.62/2.29.

In these diagrams the clusters are distributed over the loci defined by giant stars (cf. Fig. 5c Origlia et al. 1993). The warmer and less metallic systems are at the bottom left while cooler and more metallic ones progressively move up and to the right. There is general agreement between the metallicities given in Figure 1 (taken from Zinn 1985) and the trend in Figure 2 but with a few remarkable exceptions: Ter 5 ($[\text{Fe}/\text{H}] = +0.24$, the highest value in our sample) appears to be much warmer than NGC 6440 ($[\text{Fe}/\text{H}] = -0.26$) and other clusters of lower



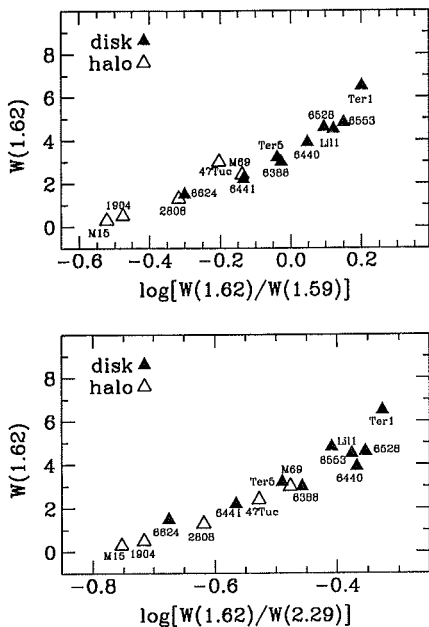


Figure 2: Spectroscopic 1.62 vs 1.62/1.59 and 1.62 vs 1.62/2.29 colour-magnitude diagrams.

metallicities while NGC 6553 ([Fe/H] = -0.28) seems to be as cold as clusters with [Fe/H] > 0 (NGC 6528, Lil 1). Unless this is due to large anomalies in the C/Fe and Si/Fe abundances, this probably demonstrates that our IR indices provide a more precise measurement of [Fe/H] in high metallicity systems. The same conclusion can be drawn from the plots of spectroscopic indices versus [Fe/H] in Figure 3 which show a scatter at large metallicities which is considerably in excess of the measurement accuracy.

We are now studying the possible

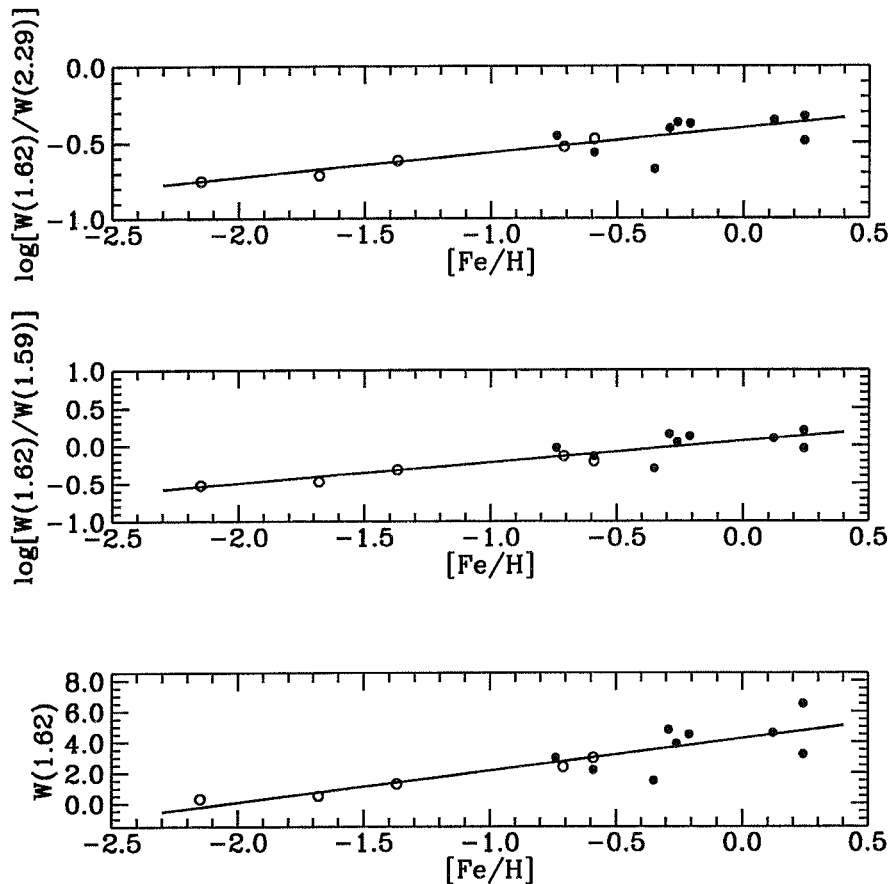


Figure 3: Correlation between the 1.62, 1.62/1.59 and 1.62/2.29 indices with the metallicities reported by Zinn (1985). Open circles are the halo clusters and filled ones are the disk+bulge clusters.

effects of C/Fe and Si/Fe anomalies using synthetic spectra based on model stellar atmospheres before producing a precise metallicity scale on diagrams like those in Figures 2 and 3.

4. References

Chiosi C., Bertelli G., Bressan A., Nasi E.: 1986 *Astron. Astrophys.* **165**, 84.

Frogel J.A., Persson S.E., Cohen, J.G.: 1983a, *Astrophys. J. Suppl.* **53**, 713.
 Frogel J.A., Cohen, J.G., Persson S.E.: 1983b, *Astrophys. J.* **275**, 773.
 Origlia L., Moorwood A.F.M., Oliva E.: 1993, *Astron. Astrophys.* **280**, 536.
 Renzini A., Buzzoni A., 1986: *Spectral Evolution of Galaxies*, eds. C. Chiosi and A. Renzini, p. 195.
 Zinn R.J.: 1985, *Astrophys. J.* **293**, 324.

Probing Dust Around Main-Sequence Stars with TIMMI

P.O. LAGAGE and E. PANTIN, SAp/DAPNIA, CE Saclay, France

The search for extra-solar planetary systems is a fascinating challenge. Direct imaging of such planets is hopeless, at least nowadays, so that efforts have been focused on looking for possible effects induced by a planet on its host star, such as faint modulation of the apparent flux (Paresce 1992 and references therein) or modulation of the apparent period in case of pulsars (Wolszczan and Frail 1992); but these searches are difficult. Since the discov-

ery by IRAS in 1984, that many main-sequence stars are surrounded by dust (Aumann et al. 1984, review by Backman and Paresce 1993 and references therein), it has been recognized that gravitational perturbations of dust orbits by a planet could result in large modifications of the dust structure, such as voids of matter in the region inside the planet orbit or asymmetries (for example, Roque et al., in press). That is why many telescopes have been pointed to-

wards main-sequence stars with IR excess, in an attempt to image the dust responsible for the excess.

Up to now, only the dust around the β -Pictoris star has been unquestionably imaged, thanks to visible observations (Smith and Terrile 1984). The dust was shown to be in a disk-like structure. But even with sophisticated techniques, using coronagraphic adaptive optics or antiblooming CCDs, the region inside a radius of 2.5'' (40 AU at the distance of